VAULT-FILL INTERACTION IN MASONRY BRIDGES: AN EXPERIMENTAL APPROACH - 2: DYNAMICS

A. Brencich, G. Riotto

University of Genoa, Department of Civil, Chemical and Environmental Engineering, Genoa, ITALY.

e-mails: brencich@dicca.unige.it, giuseppe.riotto@unige.it

SUMMARY

This paper is the continuation of a companion paper presented in this conference by the same authors. It is first demonstrated that scaled models may reproduce the dynamic response of masonry bridges if proper scaling criteria are set. The comparison of the natural frequencies of the real bridge to the ones expected on the basis of structural models may provide important information on the inner structure of the bridge, which is often known only approximately or is unknown at all and is only postulated. A series of laboratory tests are discussed to identify and quantify the contributions to the natural modes, shapes and frequencies of the different elements of a masonry bridge. 1:4 prototypes have been used; dynamic tests have been performed at different levels of load-induced damage and in different settings: bare arch and arch + fill. It is showed that the structural elements, and their effective contribution to the load bearing structure, may actually be identified by means of dynamic identification techniques. Damages, mainly due to material degradation or overload, instead, may be identified on the basis of dynamic testing only if their extent is large enough to be detected also visually.

Keywords: *Masonry bridges, load carrying structure, arch-fill interaction, deep arch, shallow arch.*

1. INTRODUCTION

A large part of bridges in the European transportation system consist of masonry structures. Material degradation, but also increasing loads and speed ask their assessment through reliable procedures. Theoretical and experimental research of the last thirty years mainly refer to the static response of masonry bridges [1-7] and ask some simplifying assumptions either in the geometry and in the constitutive models for the materials. Even though 3D FEM models overcome some of these limitations, they still ask simplified approaches to several issues such as when modeling brickwork and interfaces. Consequently, some aspects of the mechanical response of masonry bridges is still partially unknown, among which the actual contribution of spandrels and fill to the load bearing structure.

Dynamic testing has been recently applied to masonry bridges aiming at the identification of the natural frequencies and modes of the bridge to verify the reliability of the mechanical models for structural analysis [8, 9]. A limited number of tests has been performed till now due to practical difficulties so that a comprehensive view of the dynamic response of masonry bridges is not yet common to the community of engineers.

Among the crucial issues raised by dynamic testing but still obscure, damping is of primary importance since it plays a crucial role in Seismic Engineering.

The practical difficulties in performing tests on real bridges have been overcome by reduced scale testing. A quite large series of tests has been performed at Bolton Institute [6] on models with geometric ratio 1:5-1:4. Since modern ordinary brickwork (engineering blocks) was used in the models, the material strength was not scaled so that the similarity with real prototypes was lost. Other reduced scale tests increased the weight by centrifuge testing; in this case the similarity with the prototype was not lost but other technical difficulties were encountered during the tests and no dynamic test could however be performed [10].

In this paper, reduced scale bridge models are considered, retaining the similarity with the prototype bridges by means of an approx. 1:4 reduced material strength. Static (companion paper in this conference) and dynamic tests (this paper) allow some discussion on the contribution of some "non-structural" elements, such as the fill, and provide a first parametric data base.

2. MODEL-TO-PROTOTYPE SIMILARITY

In order to retain the similarity to the prototype, we recall the Π (or Buckingam) Theorem [11]: natural frequencies f depend on: i) material stiffness E; ii) arch span l, iii) material density ρ; iv) area A of the cross section (geometric stiffness). Assuming E, l and ρ as governing parameters (A is a geometric parameter which units can be cosnidered as derived from the geometric governing parameter l), the following dimensional equation holds:

$$[f] = [l]^{1} [\rho]^{-1/2} [E]^{1/2} \tag{1}$$

Asuming α the geometric, β the material stiffness, γ the density and δ the frequency model-to-prototype ratios, eq. (1), that is very similar to the classical form of the natural frequency of an elastic SDOF, shows that similarity with the prototype is achieved if the scale ratios satisfy the following condition:

$$\delta = \alpha \, \beta^{1/2} \gamma^{-1/2} \tag{2}$$

Eq. (2) provides the frequency model-to-prototype ratio as a function of the ratios of the governing parameters. To retain similarity in static tests, the material strength of the model should be reduced the same amount as the geometric ratio. For this reason, the voussoiers of the model arches consist of aerated autoclaved concrete with mechanical properties of table 1 and compared to average values for masonry bridges [8]. The fill used in the tests consists of a pure granular material graded 8-10mm. Eq. (2) shows that the model-to-prototype frequency ratio is expected to be 0.42, i.e. the natural frequencies measured in the tests are expected to be 0.42 times the actual values. Models with fill exhibit a model-to-prototype ratio on the weight of 4/5 since the volume of the fill is 2.2 times the volume of the arch. This leads, from eq. (2), to a frequency model-to-prototype ratio equal to 0.29. The similitude ratios allow the extension of the results to real prototypes; in addition, the tests show the effect of "non structural" elements on the basic dynamic properties of masonry arch bridges: natural frequencies and natural modes.

The arches were built assembling pre-cut blocks without mortar. Steel chains were used to lock the springing of the arches.

The tests discussed in this paper are a part only of a wider testing program where also arches with spandrels are taken into account and where the load distribution inside the fill is taken into account, too. This belong to the final part of the research.

Table 1. *Material properties (aerated autoclaved concrete, brickwork, fill).*

Property	Average	Model C.O.V.	Std. Dev.	Prototype	model/ /prototype
Compr. strength f_c [MPa]	<2.9>	12 %	0.35	11.6	1 / 4
Compr. elastic modulus E [MPa]	<500 >	18 %	90	2000	1 / 4
Density ρ a.a. concrete [kN/m^3]	<6.4 >	4%	0.25	18	1/2.8 shallow
Density ρ fill [kN/m^3]	<17 >	3%	0.51	17	3/4 deep
Internal friction angle - fill	32°	8%	2.64	/	/

3. MODELS, EXPERIMENTAL SETUP AND DATA ANALYSIS

3.1. Models

Two models have been considered with rise-to-span ratio =0.2 and 0.3 respectively, spanning 4m, 25cm thick and 45cm deep, represented in figure 1 (fill is not represented). These two geometries are intended to be 1:4 scaled models. Two model types have been tested: i) arch only; ii) arch + fill.

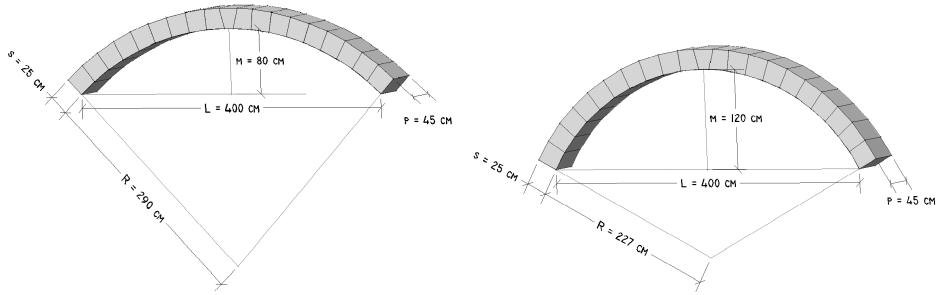

Fig. 1. *a) Shallow arch. r/s =0.2. b) Deep arch. r/s=0.3.*

The accelerometers used for the dynamic identification of the arches have been located in the positions showed in figure 2. Three different testing setups were used in which the position of the sensors indicated with 1, 2 and 3 was kept unchanged while the other were moved to record a larger number of data. The locations of the accelerometers aimed at the identification of: i) symmetric modes; ii) anti-simmetric modes; iii) torsional modes, if any.

3.2. Testing procedure and identification technique

Any arch was excited with a non-instrumented hammer in different points along the structure. The excitation points were located near the fixed sensor for activating the largest possible number of modes; besides, in all the cases where some kind of damage had been produced in the arch (by the static load tests) the setup allowed the identification of local modes that could arise (as they actually did) in these cases. This occurrence has been showed by [12] on masonry models of ordinary buildings where the extensive damage that precedes the collapse has been found to be coupled with the activation of local modes that were not present in the undamaged structure. The hammer impact loading has been chosen following previous work [13] on the nonlinear dynamic response of some classes of materials such as masonry.

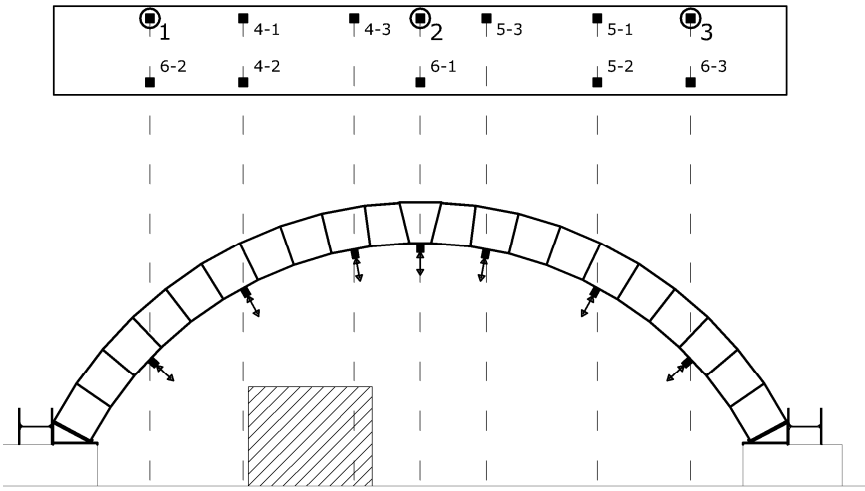

Fig. 2. *Location of the accelerometers.*

The Frequency Domain Decomposition [14] was used as identification technique. The auto- and the cross-Power Spectral Density (PSD) were obtained from the acceleration data registered. In this way it was possible to form the PSD matrix $\mathbf{S}_{xx}(\omega)$. For any values of ω a Singular Value Decomposition of the PSD matrix. was performed and the singular values σ and the singular vector $\mathbf{v}$ were obtained.

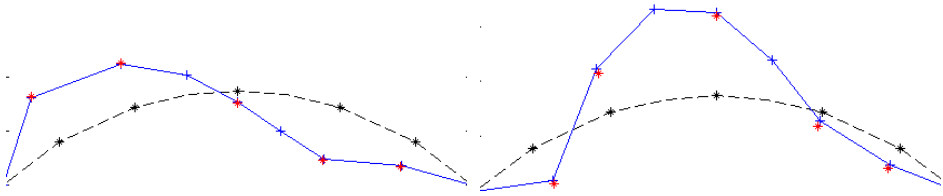

Fig. 3. *Left - Shallow arch - Mode 1 – 10.3 Hz, right - Shallow arch - Mode 2 - 16.6 Hz.*

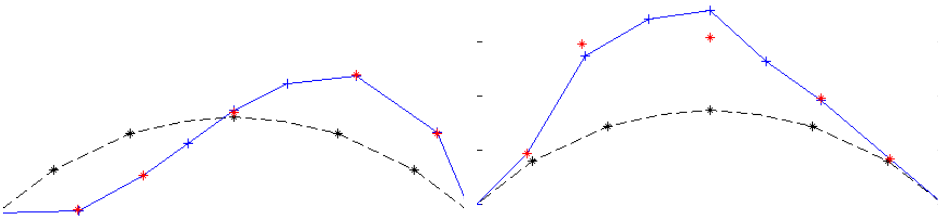

Fig. 4. *Left - Shallow arch + Fill - Mode 1 - 20.0 Hz, right - Shallow arch - Mode 3 - 25.6 Hz.*

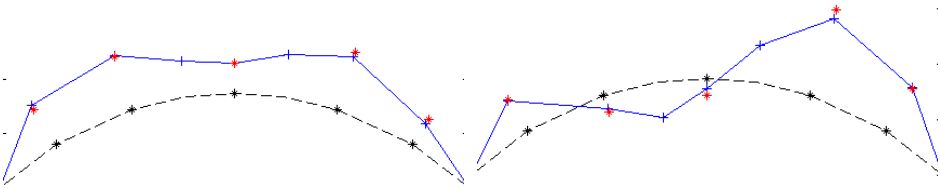

Fig. 5. *Shallow arch + Fill - Mode 2 - 32.5 Hz, right - Shallow arch + Fill - Mode 3 - 42.2 Hz.*

Under the conditions discussed in some recent works [15], in a neighbourhood of the resonances, the PSD of the principal coordinates of the structure can be identified by the singular values σ and the natural modal shapes by the singular vectors **v**. Even if the condition is not perfectly fulfilled, the adopted technique gives reliable results due to its robustness.

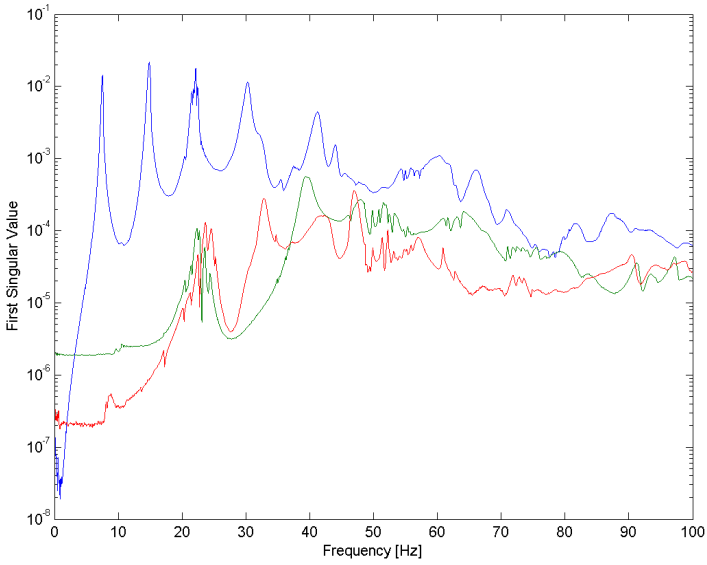

Fig. 6. *Singular values for the shallow arch n. 2: bare arch=blue line; arch + fill=green line; arch + fill+damage = red line.*

4. TEST RESULTS

4.1. Shallow arch

Figures 3 and 4 show the first three natural modes of the shallow arch models for the bare arch, Fig. 3, and for the model with the fill, figure 4; Red and black dots are related to accelerometers located in the same section of the arch but on opposite sides in order to verify possible torsional modes of the arch so that if red and black dots coincide, torsional effects were not present due to good contact between adjacent blocks. Since the natural modes are common to all the models, they are plotted for arch 1 only. Figure 5 shows the singular values diagram for the bare arch (blue line), for the model with the fill (green line) and for the arch with fill and damage (red line) where the peaks correspond to a natural frequency. Table 2 summarizes the frequencies and modal forms for all the three shallow models considered.

Table 2. *Frequencies and modes for the shallow arch. Bare arch and arch+fill models.*

		Mode 1 ***Frequency [Hz]***	**Mode 2** ***Frequency [Hz]***	**Mode 3** ***Frequency [Hz]***	**Mode 4** ***Frequency [Hz]***
Arch 1	Bare arch	10.3 Emi-symm.	16.6 Symm.	25.6 Symm.	/
	Arch + Fill	20.0 Emi-symm.	32.5 Symm.	42.2 Symm.	
Arch 2	Bare arch	7.6 Emi-symm.	14.9 Symm.	22.5 Symm.	30.5 Emi-symm.
	Arch + Fill	22.3 Emi-symm.	39.3 Symm.	47.9 Symm.	
	Arch + Fill + damage	23.7 Emi-symm.	32.7 Symm.	40.8 Local mode	47.1 Symm
Arch 3	Bare arch	7.1 Emi-symm.	14.1 Symm.	22.5 Symm.	
	Arch + Fill	17.8 Emi-symm.	27.3 Symm.	42.6 Symm.	

Model 2 has been unloaded after the peak load when the load-displacement curve was far after the peak load and when damage in the block just below the load was severe, Fig. 6a and 6b. The unloaded arch has been identified by means of the same testing procedure already described for the other arches to estimate the effect of severe damage; the damaged model had the fill over the arch.

Figures 3 and 4 and table 2 show that:

1) the first mode is always emi-symmetric;
2) the fill rises the frequency 2-to-3 times for the first mode, 2 times for the second mode and 1.5-to-2 times for the third mode;
3) severe damage changes the natural frequencies some 20% and made evident a new mode at 40.8 Hz (Fig. 7), possible originated by some cross-over effect still under investigation. Fig. 7a shows the load-displacement curve for the damaged arch and Fig. 7b the damage below the load that characterizes the "damaged" arch.

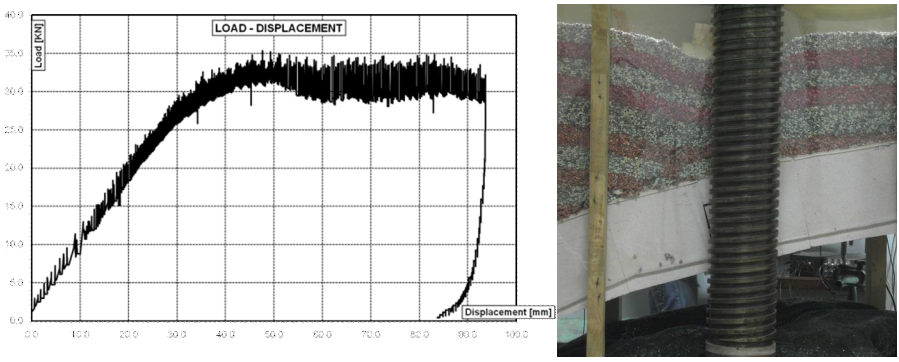

Fig. 7. *Left - Load displacement curve for shallow arch 2. Load at 1/3rd of the span; right - severe damage below the load for arch 2.*

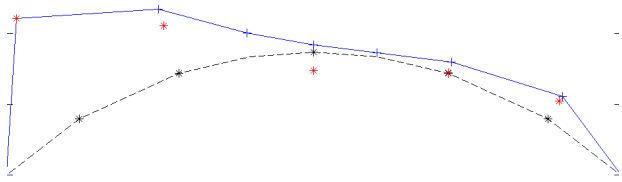

Fig. 8. *Local mode for the damaged arch - 40.8 Hz.*

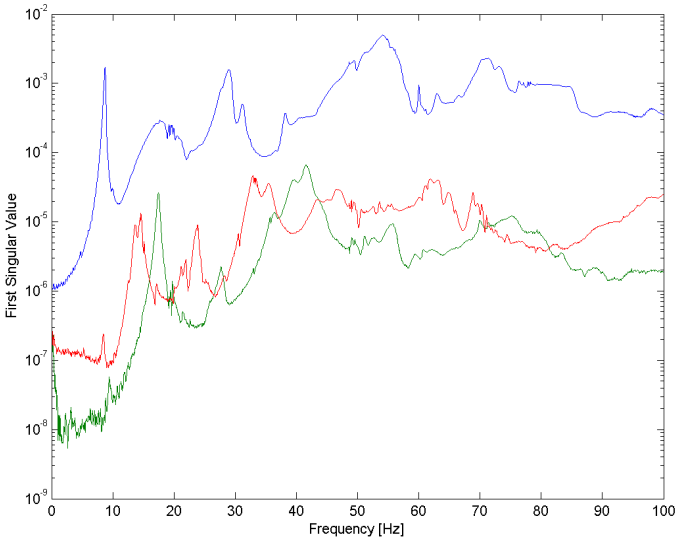

Fig. 9. *Singular values for the deep arch n. 4: bare arch=blue line; arch + fill=green line; arch + fill + damage = red line.*

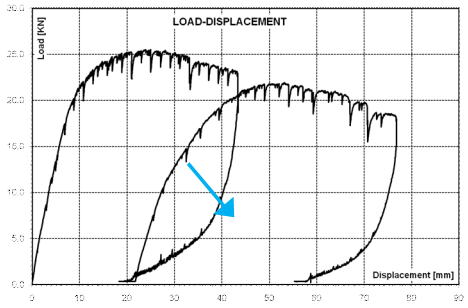

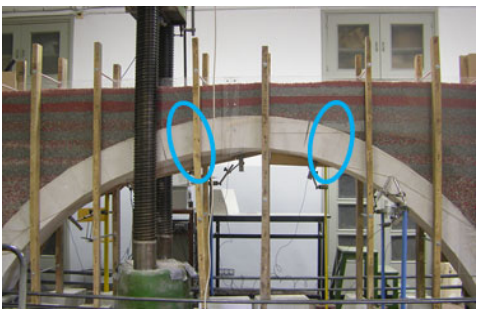

Fig. 10. *Left - Load displacement curve for deep arch 4. Load at 1/3rd of the span, right - Damage for deep arch 4.*

4.2. Deep arch

The shape of the natural modes of the deep arch, either bare and with the fill, are qualitatively the same as for the shallow arch, Fig. 3 and 4. Table 3 summarizes the test data for this geometry. Some bare arches could not be identified before the fill were placed due to practical problems with the equipment. The damaged arch is identified in Fig. 9a and 9b by the load-displacement curve and by a global image of the damaged arch.

Table 3. *Frequencies and modes for the deep arch. Bare arch and arch+fill models.*

		Mode 1 ***Frequency [Hz]***	**Mode 2** ***Frequency [Hz]***	**Mode 3** ***Frequency [Hz]***	**Mode 4** ***Frequency [Hz]***
Arch 1	Bare arch	9.8 Emi-symm.	19.3 Symm.		/
	Arch + Fill	15.9 Emi-symm.	31.5 Symm.	36.9 Symm.	
Arch 2	Bare arch	/	/	/	/
	Arch + Fill	18.5 Emi-symm.	26.1 Symm.	38.3 Symm.	42.3 Symm.
	Arch + Fill + damage	21.5 Emi-symm.	33.5 Symm.	37.7 Symm.	
Arch 3	Bare arch	/	/	/	/
	Arch + Fill	17.3 Emi-symm.	29.7 Symm.	39.4 Symm.	42.3 Symm.
	Arch + Fill + damage	13.9 Emi-symm.	21.2 Symm.	32.6 New mode	35.8 New mode
Arch 4	Bare arch	8.8 Emi-symm.	15.8 Symm.	29.4 Emi-symm.	
	Arch + Fill	17.5 Emi-symm.	29.1 Symm.	41.7 Symm.	
	Arch + Fill + damage	14.6 Emi-symm.	23.6 Symm.	32.9 New mode	35.5 New mode

Table 3 shows conclusions similar to the previous case. Due to the low level of the axial thrust of a deep arch, the differences from one arch to another is here ascribed to the irregularities on the contact surface between adjacent blocks. The effect of fill and of damage are analogous to what already discussed for the shallow arch. The trend in natural frequencies due to severe damage is here not so clear as for the previous case since a trend for decreasing frequency with damage is typical of several arches but for one case in which damage induced an increase of the frequencies; this feature is still under consideration and no reason has yet been identified. What is common to the preceding case is that some new local mode, possibly originated by some cross-over phenomenon, appears in damaged arches, Fig. 10.

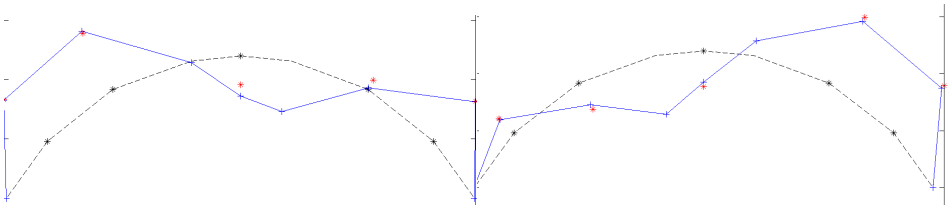

Fig. 10. *Left - New mode for the damaged arch - 32.6 Hz, right - New mode for the damaged arch - 35.8 Hz.*

5. DISCUSSION

The dynamic tests performed on reduced scale models of masonry arches provided some information on the effect of fill and damage on the dynamic properties of masonry arches. The model-to-prototype ratio is discussed in section 2 so that the extension to real cases is possible.

Even though some aspects are still not clear, we can say that the bare arch and the arch with the fill are substantially different structures. Also from the dynamic point of view, as already conjectured from static load tests and from theoretical work, the fill changes the response of the arch in a fundamental way.

The effect of damage can be addressed generally as a reduction of stiffness and, therefore, as a reduction of the natural frequencies. Nevertheless, we have to outline that only severe damage can be noticed from dynamic identification since damage is a typical local phenomenon while natural frequencies and models are global quantities that are affected by local damage only if the damage is severe. Moderate damage will probably induce reduced change in structural frequencies that could be shadowed by the errors in dynamic identification.

In the case of arches with fill the natural modes appear to be non-symmetric. This is due to the lateral structures used for containing the fill that are not rigid and, as such, affect the dynamic properties of the arch. Nevertheless, it appears that this effect plays a minor role on the overall dynamic response of the model.

The research is still going on and several other arches, also with spandrel, are being tested so that more general conclusions will be derived in the next future.

REFERENCES

[1] HEYMAN J., *The masonry arch*, Chichester, Ellis Horwood, 1982.

[2] PAGE J., Load tests to collapse on two arch bridges at Preston, Shropshire and Prestwood, Staffordshire, *Dep. of Transport, TRRL Res. Report 110, TRL,* Crowthorne, England, 1987.

[3] HARVEY A.W., The application of the mechanism analysis to masonry arches, *The Str. Eng*., 66, pp. 77-84, 1988.

[4] HUGHES T.G., Analysis and assessment of twin-span masonry arch bridges. *Proc. Inst. of Civil Eng.rs*, 110, pp. 373-382, 1995.

[5] MELBOURNE C., BEGIMIL M., WEEKES L. The load test to collapse of a 5m span brickwork flat arch barrel, *Proc. I Int. Arch Bridge Conf.*, Thomas Telford, London, 1995.

[6] MELBOURNE C., GILBERT M. and WAGSTAFFF M., The collapse behaviour of multi-span brickwork arch bridges, *The Str. Eng.*, 75, pp. 297-305, 1997.

[7] HUGHES T.G., BLACKLER M.J. A review of the UK masonry arch assessment methods, *Proc. Inst. of Civil Eng.rs*, 122, pp. 305-315, 1997.

[8] BRENCICH A., SABIA D. Experimental identification of a multi-span masonry bridge: the "Tanaro Bridge", *Constr. & Build. Mat.s*, 22 (10), pp. 2087-2099, 2008.

[9] BRENCICH A., SABIA D., *Structural identification of masonry arch bridges*, Proc. ICOMAC '09.

[10] DAVIES M.C.R. HUGHES T.G., TAUNTON P.R. Centrifuge testing of model masonry arch bridges. *Proc. of the Institution of Civil Engineers –Geotechnical Engineering*, 1998, Vol. 131, no. 3, pp. 141-145.

[11] BARENBLATT G.I., *Dimensional Analysis,* Gordon and Breach Science Publishers, New York, 1987.

[12] BENI F., LAGOMARSINO S., MARAZZI F., MAGONETTE G., PODESTA' S., Structural Monitoring through Dynamic Identification, *Proc. of 3rd World Conf. on Str. Control* (Como, Italy, April 2002), 3: pp. 139-146, 2002.

[13] PODESTA' S., RIOTTO G., MARAZZI F., Reliability of dynamic identification techniques connected to structural monitoring of monumental buildings, *Str. Contr. & Health Mon*, 15, pp. 622-641, 2008.

[14] BRINCKER R., ZHANG L., ANDERSEN P., Modal identification of output-only systems using frequency et al., domain decomposition, *Smart Mater. & Struct*., 10, pp. 441-445, 2001.

[15] CARASSALE L., PERCIVALE F., Frequency-domain output-only identification of linear structures subject to stationary excitation, *Proc. 5th Int. Conf. on Comp. Stochastic Mech.*, Rhodes, Greece, pp. 147-156, 2006.